Simulation of the Radar Cross-Section of Dynamic Human Motions Using Virtual Reality Data and Ray Tracing

Akash Deep Singh, Shobha Sundar Ram and Shelly Vishwakarma
Indraprastha Institute of Information Technology Delhi
New Delhi, India 110020
{akash14131, shobha and shellyv}@iiitd.ac.in

***Abstract*—Radar returns from dynamic human motions are usually modeled using primitive based techniques. While the method is computationally simple and reasonably accurate in generating micro-Doppler signatures of humans, it is unreliable for predicting the radar cross-section (RCS) of the human especially at high frequencies. On the other hand, the shooting and bouncing ray method is effective for accurately measuring the RCS of humans. However, it has been carried out for only a single aspect or posture of the human. In this work, we present a method to simulate the radar cross-section of dynamic human motions across multiple postures by combining virtual reality data with shooting and bouncing ray (SBR) techniques. We convert each frame of human motion capture data to a poly-mesh structure of a human body and then incorporate the SBR technique for computing the resulting RCS. We verify the simulated results with measurement data at 24GHz.**

I. Introduction

Radars have been increasingly used, over the last decade, to detect and track human activities for a variety of applications. These include indoor radars for security and surveillance purposes [1], [2] or for biomedical applications such as fall detection [3] and ground penetrative radar for search and rescue operations [4]. These applications have typically used radars operating at frequencies below the X band to enable through-wall or ground penetration. Alternatively, radars have been employed in outdoor line-of-sight environments for automotive applications (26 GHz or 77GHz) [5]. In all of these cases, the detection and estimation performance of the radar could be enhanced with an accurate prediction of the radar cross-section (RCS) of the human. The RCS is a function of the frequency, polarization, aspect angle of the radar and the shape and material characteristics of the target. Currently, coarse estimates of the human RCS are available from measurement studies at specific frequency bands of interest [6]. An accurate simulation model of the RCS of humans across diverse radar operating conditions and across dynamic human motions would facilitate the rapid development of automatic target detection and recognition algorithms.

There are however some challenges for obtaining the RCS of humans compared to other types of radar targets. For one, the human is a non-rigid body which undergoes a variety of dynamic motions. Therefore, there is a lot of variation in the RCS based on each distinct human posture and aspect with respect to the radar. Secondly, the human is a multi-layer dielectric body. Additionally, there may be significant variation arising from the roughness of the surface due to skin and clothes. While several studies have been carried out to study the specific absorption rate (SAR) of microwave frequencies in human tissues, these studies have been restricted to only specific portions of the human body at microwave frequencies [7]. The RCS of complex targets are usually modeled using computational electromagnetic techniques such as finite element methods (FEM), method of moments (MOM) or finite difference time domain techniques (FDTD). However, none of these techniques are suitable for simulating the RCS of a human due to their high computational complexity and the large three dimensional spatial extent of the human with respect to the radar wavelength. Alternately, the RCS of humans have been predicted using the computationally simple primitive based techniques [8]. Here, the different body parts are modeled as simple primitives such as ellipsoids, spheres or cylinders whose RCS are well characterized. The RCS of the human is assumed to be the complex sum of the RCS of these simple shapes. While this technique has been used extensively in recent literature to model the micro-Doppler signatures of human motions [8], it is an unreliable tool for predicting the RCS of the human body especially at high frequencies. Additionally, the technique does not capture the entire phenomenology of the electromagnetic scattering off humans such as the shadowing of some body parts by the others, multiple scattering etc. In [9], Dogaru used the computational electromagnetic software, Xpatch, based on the shooting and bouncing ray technique (SBR) [10] to model the radar returns of humans at X band frequencies. SBR is based on a combination of geometric optics (GO) and physical optics (PO) and has been extensively used to model the RCS of complex targets especially at high frequencies (above X band). Dogaru's work was restricted to the simulation of the RCS of a single human for a few postures.

In this paper, we propose a method to accurately predict the RCS of dynamic human motions by combining SBR with computer animation models of the human motion. The animation motion may be readily availed from motion capture databases such as [11] or [12]. Alternately, the motion data may be captured in real time using the Kinect sensor as proposed by [13]. We choose the second method in order to collect synchronized simulation and measurement data. The output of the motion capture process is motion information of a stick figure or skeletal model of the human. We embody the stick figure with a realistic human body using an animation

978-1-5386-4167-5/18/$31.00 ©2018 IEEE

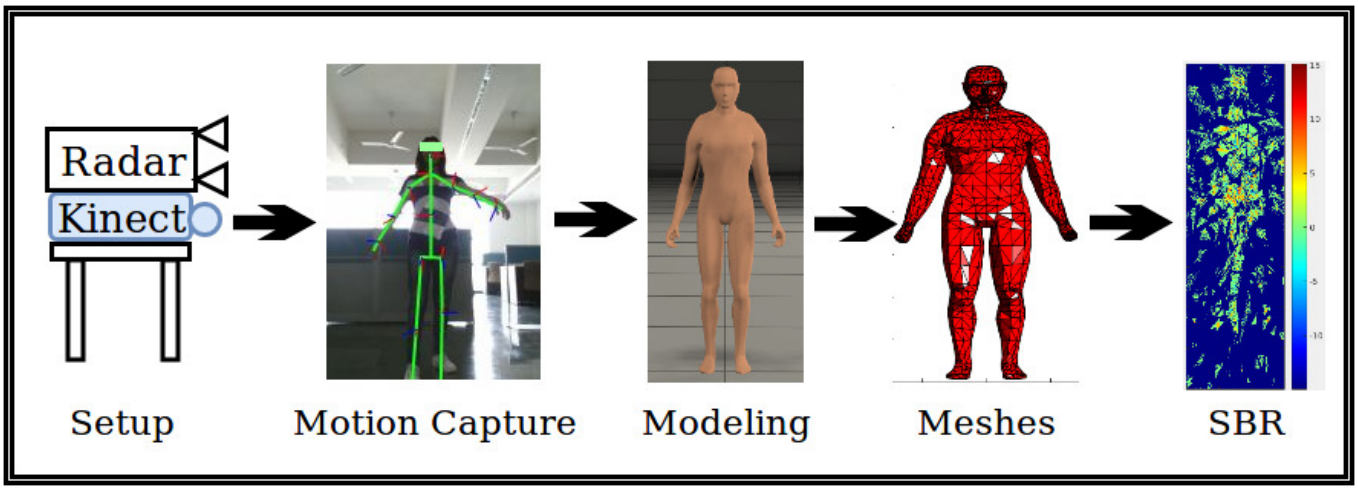

Fig. 1: Simulation Methodology - motion capture by Kinect provides skeletal / stick figure motion model of human. This is converted to a realistic body model using Poser from which the body surface is meshed with triangles. Finally, we compute the backscattered electric field based on the scattered rays from the poly-meshed human on an aperture plane.

software called Poser from Smith Micro Inc. Then we render the realistic body image with a mesh of triangles. Finally, we implement the SBR suggested in [10] on this poly-mesh human to generate the backscattered field by the human towards the radar. While the computational complexity of the proposed method is significantly higher than the simpler primitive based technique, we demonstrate that the RCS prediction is far more accurate. We finally validate our results using measurement data gathered from a 24 GHz radar developed by Ancortek Inc. for multiple frames of human motions.

The paper is organized as follows. In the following section, we describe the simulation methodology. Then in Section III, we describe the experimental set up used for gathering the data. Finally, in Section IV, we present the results of the simulation.

II. Simulation of RCS of Humans Using Shooting and Bouncing Ray Techniques

In this section, we present the method to hybridize the electromagnetic modeling of the radar scatterings off the human with the animation data. Fig.1 shows the steps. The first step is to capture animation motion of the humans. There are several existing motion capture databases such as [11] and [12] which provide animation models of human motions. Earlier works have extensively used these databases to simulate micro-Doppler signatures of humans [8]. These databases offer the advantages of high quality motion capture data for realistic human motions. Alternately, motion capture data can be gathered using a cheaper alternative as proposed by [14] using the Kinect sensor. In this work, we use the second technique to generate motion capture data so as to obtain synchronized measurement and simulation data as shown in Fig.1. However, the proposed technique can be extended to any standard motion capture data.

Kinect v2 is a motion sensing input device from Microsoft's Xbox gaming console. The sensor can track 25 joints on a human as shown in Fig. 2. The skeletal image generated by Kinect, is a mirror image of the actual human

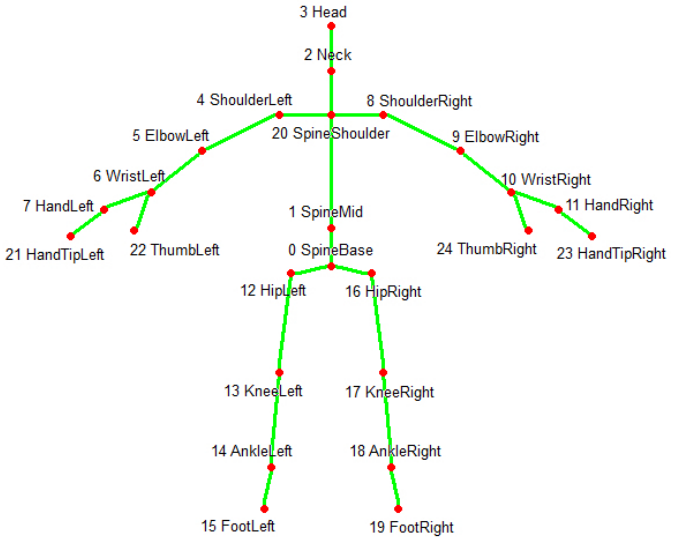

Fig. 2: Stick figure model with joint information provided by Kinect [15]

subject being tracked. The Kinect data describes the three-dimensional time-domain tracks of each of the joints of the skeleton. The sensor, however, has some limitations regarding the data collection. First, Kinect is strictly meant for detecting front facing humans. Hence, there is considerable error in the position data when the subject turns or moves away from the sensor. Second, Kinect does not accurately capture the position of the body parts that are shadowed by other parts. Finally, the sensor has a field-of-view of 0.7m to 4.4m in range and 70° in azimuth. Therefore, the motions of the humans have to be restricted within this limited field-of-view of the Kinect. The frame rate of the motion capture data is 30 frames per second. Therefore, the data are interpolated to match the high sampling frequency requirements of the radar data. The next step is to incorporate an electromagnetic model on the virtual reality

animation data. Previously in [8], a primitive based model was proposed that was computationally simple to execute and suitable for generating the scattered returns at low frequencies. We compare the results from the primitive based technique with an alternate technique based on shooting and bouncing rays.

A. Primitive Based Modeling

All of the bones connecting the joints of the human body are modeled as simple primitives - spheres, cylinders or ellipsoids. The RCS of these simple shapes are well characterized especially at high frequencies. Therefore, the RCS of the human can be estimated by the complex sum of the RCS of each of these body parts. Naturally, the accuracy of this RCS estimate is poor since these simple primitives do not capture the actual shape or size of the different body parts. Additionally, second order effects such as shadowing and multiple scattering between the body parts are not captured. However, the primitive based modeling has been extensively used to generate micro-Doppler signatures of different human motions described with animation data.

B. Ray Tracing

An alternate method is to use a combination of geometric optics and physical optics to capture the scattering physics of the human body. This method was explored for a single human posture by [9] and was demonstrated to show high accuracy especially at X band frequencies. In this paper, we provide a method to combine the animation data obtained from motion capture with the ray tracing technique used in [10].

The Kinect data describing the motion of the human joints are extracted using an inbuilt module in Poser Pro software developed by Smith Micro Software Inc. [16]. Alternately, any other motion capture data of humans, from the existing virtual reality databases, can be directly provided to Poser. The Poser has a library of human models which can be combined with the stick figure motion data to generate a meshed model of human body as shown in Fig.1. In this work, we selected the low resolution male model - a surface body model composed of mesh triangles. We exported the meshed data to MATLAB for further processing.

Our ray tracing technique is based on [10]. We assume that the human subject is standing on the XZ plane with his height along the Y axis. The human is in the far-field of the radar along the Z axis. We assume that the incident field is vertically polarized. We model the incident field as multiple parallel incident rays originating from an illumination plane, Σ_A parallel to the XY plane before the human subject. The illumination rays are equi-spaced $\frac{\lambda}{10}$ apart along both the X and Y dimensions where λ is the wavelength of the radar. We set the size of the illumination plane to be equal to the width and height of the human - the extents of the human along the X and Y axes respectively. Any point $\vec{r}_p$ on the incident ray can be defined using the parametric equation of a straight line where $\vec{r}_0$ is a reference position vector on the illumination plane, $\vec{K}$ is the direction vector of the illumination ray and t as the associated parameter (equivalent to time).

$$\vec{r}_p = \vec{r}_0 + t\vec{K} \tag{1}$$

Our objective is to determine the intersection positions of the illumination rays upon the poly-mesh human structure. Since the poly-mesh structure consists of triangles, we must determine the intersection of each illumination ray with each triangle composing the human body. The equation of the plane consisting of the three vertices $(\vec{r}_1, \vec{r}_2, \vec{r}_3)$ is given by

$$\hat{n} \cdot \vec{r}_p - \vec{r}_1 \tag{2}$$

Here $\hat{n}$ is the unit normal vector obtained from

$$\hat{n} = \frac{(\vec{r}_{31} \times \vec{r}_{32})}{|\vec{r}_{31} \times \vec{r}_{32}|} \tag{3}$$

The intersection point, $\vec{r}_p$, of the illumination ray and the plane containing the triangle is obtained from equations (1) and (2). Subsequently, we determine if $\vec{r}_p$ lies within or outside the triangle by performing some vector calculus operations. We check if $\vec{r}_{p1} \times \vec{r}_{21}$ carries the same sign as $\vec{r}_{31} \times \vec{r}_{21}$. We repeat these checks for the other two vertices as well. If the signs are alike for all three cases, then we can conclude that $\vec{r}_p$ lies within the triangle and hence the triangle is illuminated by the incident electric field. If more than one triangle on the human body are illuminated by the same illumination ray, then we consider only the triangle closest to the radar to be illuminated and assume that the other triangles are shadowed.

Next, we find the reflected ray generated from the illuminated triangle using the two conditions of Snell's law of reflection - (1) the reflected ray must lie in the plane of incidence and (2) the angle of reflection must equal the angle of incidence. Accordingly, the reflected ray can be computed as

$$\vec{R} = \vec{I} + 2(\hat{I} \cdot \hat{n})\vec{n} \tag{4}$$

where $\vec{I}$ is the incident ray given by $\vec{r}_{p0}$ and reflected ray $\vec{R}$ is given by $\vec{r}_{p+1,p}$. If the electric field of the incident ray is given by $E_0\hat{y}$, then the reflected field at any position $\vec{r}_{p+1}$ is given by

$$\vec{E}(\vec{r}_{p+1}) = (DF) \cdot \Gamma \cdot \vec{E}(\vec{r}_p) \cdot e^{-j(\phi)} \tag{5}$$

where

$$\phi = k_0 ||\vec{r}_{p+1} - \vec{r}_p|| \tag{6}$$

Here, DF is the diffraction factor which accounts for the curvature of the surface. In our case, DF is one since we have considered a planar triangular surface. Γ is the planar reflection coefficient, which can be computed from the angle of incidence and the material characteristics of the two mediums, and ϕ is the phase difference due to the path travelled from the incident ray to the outgoing reflected ray. The scattered rays off the body may interact with other parts of the body before reaching the radar. Therefore, we repeat the steps from (1) to (5) by replacing the primary illumination rays with the secondary reflected rays. This process can be repeated either till the RCS reaches convergence or till all the primary rays have returned to the aperture plane Σ_A.

In order to compute the backscattered field on the radar, we trace the position and strength of the reflected rays reaching the aperture plane Σ_A. Note that while the illumination rays were equi-spaced along the illumination aperture, the scattered rays may not be uniformly distributed along the backscatter aperture as shown in Fig.1. The final monostatic RCS is computed by

$$RCS = 4\pi ||A_y||^2 \tag{7}$$

where A_y is given by

$$A_y = \frac{jk_0}{2\pi} \int \int_{\sum_A} e^{jk_0(K_x x + K_y y)} \cdot E(x,y) sin\phi^i \cdot dxdy \quad (8)$$

Here, the strength of the field, $E(x,y)$, at the grid positions of the aperture is computed by performing two-dimensional nearest neighbour based interpolation. The entire ray tracing operation was coded in MATLAB. The code was run on a High Performance Computing (HPC) server with 40 cores and 96 GB RAM. The code took around 7 hours to run for each frame.

III. Experimental Set Up

In this section, we describe the experimental set up for simultaneously gathering simulation and measurement data. A human subject walks before the radar-Kinect setup between $1m$ to $4m$ for a duration of 5 seconds. We consider two continuous wave radars for this experiment. All the measurements are conducted in indoor line-of-sight conditions.

The first set up, shown in Fig.3, consists of a two-port vector network analyzer N9926A, configured to make time-domain S_{21} measurements at 5GHz and two linearly polarized broadband horn antennas (HF907) connected to its two ports. The two antennas act as the transmitter and receiver. The scattered signal off a human subject, moving before the radar, is captured by the the VNA, where it is amplified, inphase-quadrature (IQ) demodulated and digitized. Finally, the complex VNA measurements are downloaded to a laptop where they are further processed. The transmitted power is $3dBm$ and the sampling frequency in the receiver is $370Hz$.

The second set up, shown in Fig.3, consists of the Ancortek radar for capturing electromagnetic radar scatterings of a human subject. The Ancortek radar is built on a software defined radio platform (SDR-KIT 2400AD2) consisting of a transmitter and a dual receiver-channel operating at a center frequency of $24GHz$. The sensor consists of two high gain horn antennas for transmission and reception. We configured the radar to a continuous wave setting. The transmitted power from the radar setup is $+16dBm$. The sampling frequency of the measurement data is $128KHz$ which is decimated to $2000Hz$ while processing.

In both cases, the radar and Kinect sensor are used to simultaneously capture human animation data and electromagnetic radar scattered data. In order to compare the measurement and simulation data, both the Kinect and the radar must be synchronized. Fig.4 shows the system architecture of the synchronization system that we implemented. The radar and Kinect are each controlled by a graphical user interface on separate laptops, each configured with a Django server. Upon receiving an instruction from an Android application, both laptops use a python library "PyAutoGUI" to fire their respective GUIs to initiate data collection. Suitable delays are incorporated in the instruction to ensure that the data collection happens simultaneously.

IV. Results

First, we consider the micro-Doppler spectrograms generated from the measurement data from the two radars. We compare these results with simulated micro-Doppler spectrograms obtained from primitive based modeling. The strength of the signals of the spectrograms have been appropriately calibrated to show the RCS in dBsm. The first set of results are for 5GHz data. The micro-Doppler signatures show qualitative similarity between the measured and simulated spectrograms. The periodicity in the spectrogram arises from the swinging motion of the arms and legs as the subject walks towards the radar. The strongest signal arises from the torso which shows a positive frequency offset of approximately 40Hz corresponding to the speed of the human motion. Some negative Dopplers are also observed due to the back-swing of the limbs. Due to the low frequency and resulting low resolution, the micro-Dopplers from the different body parts considerably overlap. Next, we study the spectrograms generated from the measured and simulated data at 24GHz. Here, we observe that the higher carrier frequency has resulted in better resolution in the micro-Doppler signature. As a result, we are able to now observe individual tracks from the different body parts. The simulated spectrogram, however, shows the limitation in the primitive based technique. The primitive based modeling does not capture the effect of shadowing of a body part by another. The strength of the signal in the spectrogram which is calibrated to the RCS of the body parts shows greater deviation in the 24GHz data when compared to the 5GHz radar data.

Fig. 7 shows the measured radar cross sections for a human generated from the 24 GHz data obtained from the Ancortek Inc radar. We have also shown the RCS predicted by the primitive modeling. As anticipated, there is considerable error between the measured and predicted RCS since the primitive modeling technique does not use a realistic human body or capture second order effects such as shadowing or multipath. Therefore, the primitive modeling was a satisfactory technique for low frequency micro-Doppler signature simulation but not for high frequency RCS prediction. We also show the RCS predicted using ray tracing for several frames of the human motion. Since the ray-tracing is a computationally expensive process, we have only estimated the RCS for a few frames. However, the figure shows that the output from the ray tracing is far closer to the RCS estimate from the measurement data. The RCS values are also comparable to the values estimated from other measurement studies such as [6].

V. Conclusion

Currently the RCS of dynamic human motions have been estimated using primitive based techniques. Though computationally simple, this method is unreliable for applications requiring accurate prediction of RCS. We have demonstrated that we can generate poly-mesh human animation models that can be combined with SBR techniques to accurately predict human RCS especially at high frequencies.

References

[1] B. Carlson, E. Evans, and S. Wilson, "Search radar detection and track with the hough transform. iii. detection performance with binary integration," *IEEE transactions on Aerospace and Electronic Systems*, vol. 30, no. 1, pp. 116–125, 1994.

[2] M. G. Amin, *Through-the-wall radar imaging*. CRC press, 2016.

[3] A. Gadde, M. G. Amin, Y. D. Zhang, and F. Ahmad, "Fall detection and classifications based on time-scale radar signal characteristics," in *Proc. SPIE*, vol. 9077, 2014, p. 907712.

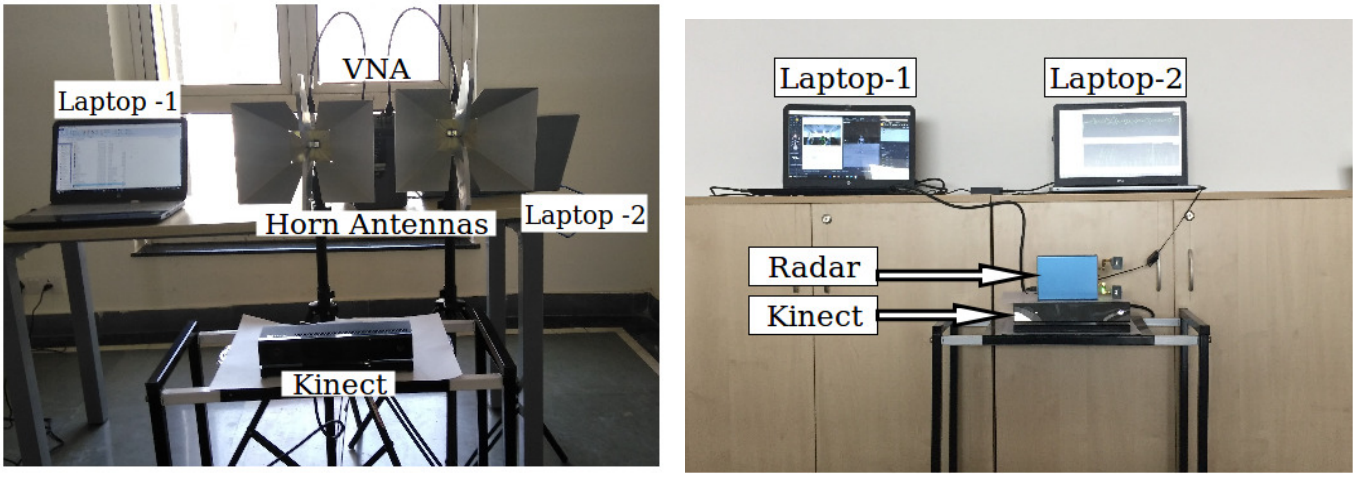

((a)) ((b))

Fig. 3: Experimental set up to simultaneously collect motion capture data using Kinect.v2 sensor and radar data at (a) 5 GHz using vector network analyzer and at (b) 24 GHz using Ancortek Inc.'s software defined radio platform

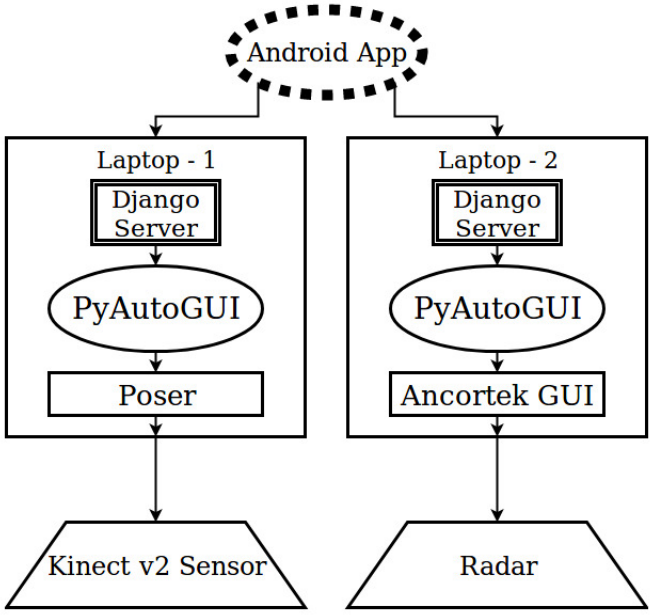

Fig. 4: System architecture for synchronizing radar and motion capture data collection

[4] A. Annan, "Ground-penetrating radar," in *Near-surface geophysics*. Society of Exploration Geophysicists, 2005, pp. 357–438.

[5] J. Hasch, E. Topak, R. Schnabel, T. Zwick, R. Weigel, and C. Waldschmidt, "Millimeter-wave technology for automotive radar sensors in the 77 ghz frequency band," *IEEE Transactions on Microwave Theory and Techniques*, vol. 60, no. 3, pp. 845–860, 2012.

[6] E. Piuzzi, P. DAtanasio, S. Pisa, E. Pittella, and A. Zambotti, "Complex radar cross section measurements of the human body for breath-activity monitoring applications," *IEEE Transactions on Instrumentation and Measurement*, vol. 64, no. 8, pp. 2247–2258, 2015.

[7] P. Bernardi, M. Cavagnaro, S. Pisa, and E. Piuzzi, "Specific absorption rate and temperature elevation in a subject exposed in the far-field of radio-frequency sources operating in the 10-900-mhz range," *IEEE Transactions on Biomedical Engineering*, vol. 50, no. 3, pp. 295–304, 2003.

[8] S. S. Ram and H. Ling, "Simulation of human microdopplers using computer animation data," in *Radar Conference, 2008. RADAR'08. IEEE*. IEEE, 2008, pp. 1–6.

[9] T. Dogaru and C. Le, "Validation of xpatch computer models for human body radar signature," ARMY RESEARCH LAB ADELPHI MD SENSORS AND ELECTRON DEVICES DIRECTORATE, Tech. Rep., 2008.

[10] H. Ling, R.-C. Chou, and S.-W. Lee, "Shooting and bouncing rays: Calculating the rcs of an arbitrarily shaped cavity," *IEEE Transactions on Antennas and propagation*, vol. 37, no. 2, pp. 194–205, 1989.

[11] "Cmu graphics lab motion capture database," http://mocap.cs.cmu.edu/.

[12] "Accad motion capture lab," https://accad.osu.edu/research/mocap/mocap_data.htm.

[13] B. Erol and S. Z. Gurbuz, "A kinect-based human micro-doppler simulator," *IEEE Aerospace and Electronic Systems Magazine*, vol. 30, no. 5, pp. 6–17, 2015.

[14] B. Erol, C. Karabacak, S. Z. Gurbuz, and A. C. Gurbuz, "Simulation of human micro-doppler signatures with kinect sensor," in *Radar Conference, 2014 IEEE*. IEEE, 2014, pp. 0863–0868.

[15] R. Hoover, "Adventures in motion capture: Using kinect data," 2016.

[16] S. M. Software, "Poser," http://my.smithmicro.com/poser-3d-animation-software.html.

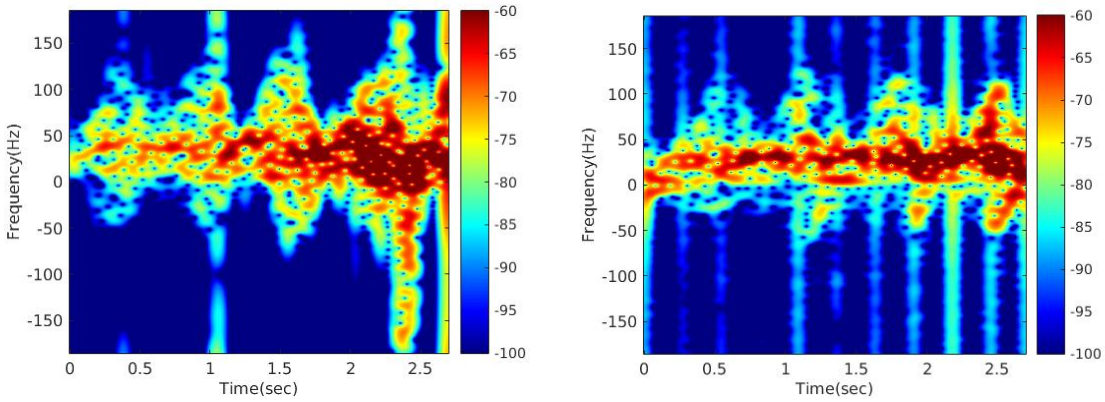

((a)) Simulated at 5 GHz ((b)) Real at 5 GHz

Fig. 5: Doppler spectrograms of RCS of humans (dBsm) at 5GHz (a) simulated from motion capture data, (b) obtained from measurement data using VNA based radar.

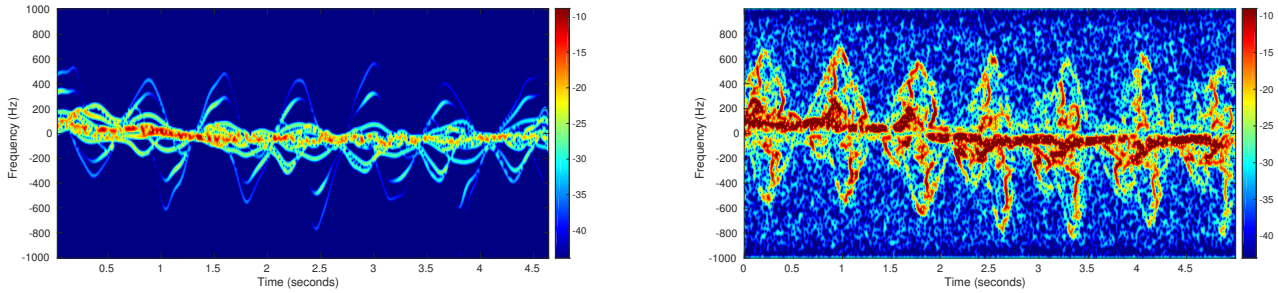

((a)) Simulated ((b)) Real

Fig. 6: Doppler spectrograms of RCS of humans (dBsm) at 24GHz (a) simulated from motion capture data, (b) obtained from measurement data using Ancortek radar.

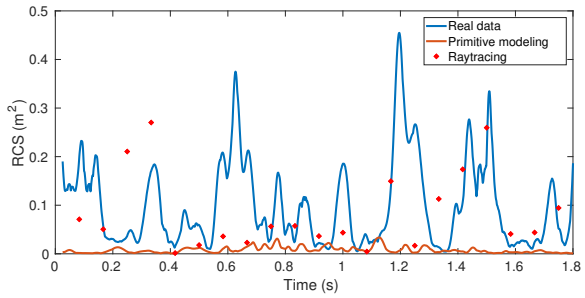

Fig. 7: Radar cross-section of dynamic human motions obtained from measurement data, from primitive based modeling and from SBR